

Reliability, Embeddedness, and Agency: A Utility-Driven Mathematical Framework for Agent-Centric AI Adoption

Faruk Alpay

Lightcap, Institut für die Zukunft

alpay@lightcap.ai

Taylan Alpay

Turkish Aeronautical Association, Aerospace Engineering

s220112602@stu.thk.edu.tr

Abstract

We formalize three design axioms for sustained adoption of agent-centric AI systems executing multi-step tasks: (A1) *Reliability* > *Novelty*; (A2) *Embed* > *Destination*; (A3) *Agency* > *Chat*. We model adoption as a sum of a decaying novelty term and a growing utility term and derive the phase conditions for troughs/overshoots with *full proofs*. We introduce: (i) an identifiability/confounding analysis for $(\alpha, \beta, N_0, U_{\max})$ with delta-method gradients; (ii) a non-monotone comparator (logistic-with-transient-bump) evaluated on the same series to provide additional model comparison; (iii) ablations over hazard families $h(\cdot)$ mapping $\Delta V \rightarrow \beta$; (iv) a multi-series benchmark (varying trough depth, noise, AR structure) reporting coverage (type-I error, power); (v) calibration of friction proxies against time-motion/survey ground truth with standard errors; (vi) residual analyses (autocorrelation and heteroskedasticity) for each fitted curve; (vii) preregistered windowing choices for pre/post estimation; **(viii) Fisher information & CRLB for (α, β) under common error models**; **(ix) microfoundations linking \mathcal{T} to (N_0, U_{\max})** ; **(x) explicit comparison to bi-logistic, double-exponential, and mixture models**; and **(xi) threshold sensitivity to C_f heterogeneity**. Figures and tables are reflowed for readability, and the bibliography restores and extends non-logistic/Bass adoption references (Gompertz, Richards, Fisher–Pry, Mansfield, Griliches, Geroski, Peres). All code and logs necessary to reproduce the synthetic analyses are embedded as LaTeX listings.

1 Background and Related Work

Diffusion and adoption. Classical S-curve models include logistic (Rogers, 1962), Bass (Bass, 1969), Gompertz (Gompertz, 1825), Richards’ generalized logistic (Richards, 1959), and substitution views (Fisher–Pry) (Fisher and Pry, 1971). Empirical literatures on diffusion emphasize timing, drivers, and parameter stability (Mansfield, 1961; Griliches, 1957; Geroski, 2000; Peres et al., 2010; Bresnahan and Trajtenberg, 1995). Recent experiments document productivity gains from generative AI (Noy and Zhang, 2023) and cautionary results about naive human–AI orchestration (Vaccaro et al., 2024; Klingbeil et al., 2024). Domain-embedded models often realize higher value (Moor et al., 2023; Pai et al., 2024; Bodnar et al., 2025), while instruction-tuning can trade off reliability (Zhou et al., 2024). HCI shows interrupt costs motivating embedding (Monsell, 2003; Czerwinski et al., 2004; Mark et al., 2008; Rubinstein et al., 2001). Trust and levels-of-automation guide the step from chat to agents (Lee and See, 2004; Parasuraman et al., 2000).

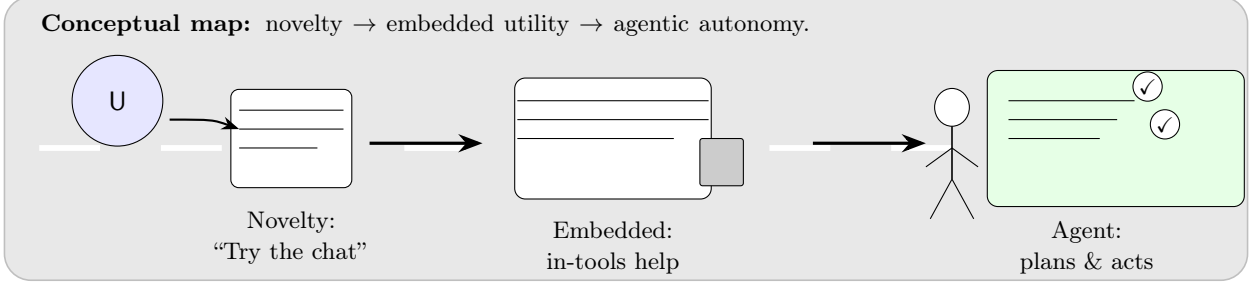


Figure 1: Street-level schematic: the user (U) first tries a novel chat, then benefits from in-place assistance inside existing tools, and finally delegates to an agent that plans and acts.

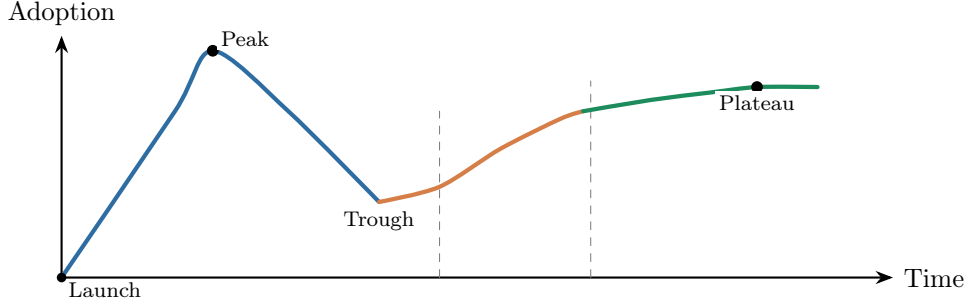


Figure 2: Adoption trajectory segmented by phases (blue/orange/green). A1–A3 shift the curve upward/rightward by increasing reliability, embedding in workflows, and enabling agentic execution.

2 Operational Definitions and Measurement

Definition 1 (Task distribution and utilities). Let \mathcal{T} be a distribution over tasks t with value-of-success $v(t) \geq 0$, base time $B(t)$, oversight time $O(t)$, and failure cost $C_f(t) \geq 0$. A system policy π acts on t .

Definition 2 (Reliability R). Reliability is

$$R(\pi) = \mathbb{E}_{t \sim \mathcal{T}} \left[\Pr_{\pi}(\text{success} \mid t) \right],$$

instantiated by domain-appropriate proper scores on an evaluation set disjoint from deployment logs.

Definition 3 (Per-task net utility and U). Given R ,

$$u_{\pi}(t) = R_{\pi}(t) v(t) - (1 - R_{\pi}(t)) C_f(t) - c_{\text{time}} \tau_{\pi}(t) - c_{\text{fric}} \phi_{\pi}(t), \quad (1)$$

where τ_{π} is time-to-completion (incl. oversight) and ϕ_{π} is context-switch/interaction cost (Sec. 5). Aggregate utility $U = \mathbb{E}[u_{\pi}(t) - u_{\pi_0}(t)]$.

Microfoundations: from \mathcal{T} to (N_0, U_{\max}) . Let $(\mathcal{T}, \mathcal{F}, \mu)$ be a finite-measure space of tasks with weight $w(t) \in [0, 1]$ proportional to task volume, $\int w(t) d\mu(t) = 1$. Define the long-run net utility improvement

$$\Delta u_{\infty}(t) := \lim_{k \rightarrow \infty} \mathbb{E}[u_{\pi}(t, k) - u_{\pi_0}(t, k)] = R_{\pi}(t) v(t) - (1 - R_{\pi}(t)) C_f(t) - c_{\text{time}} \tau_{\pi}(t) - c_{\text{fric}} \phi_{\pi}(t).$$

Assume a monotone adoption rule at the task level: an agent eventually adopts for task t iff $\Delta u_\infty(t) > 0$. Then the *utility carrying capacity* equals the mass of tasks with positive surplus:

$$U_{\max} = \int \mathbf{1}\{\Delta u_\infty(t) > 0\} w(t) d\mu(t), \quad (2)$$

or more generally $U_{\max} = \int s_\infty(\Delta u_\infty(t)) w(t) d\mu(t)$ for a smooth saturation $s_\infty \in [0, 1]$. For novelty, suppose a launch shock randomly seeds a fraction $q_0 \in [0, 1]$ of (user,task) episodes independent of Δu_∞ . With exponential abandonment hazard $\alpha > 0$, expected novelty-driven usage decays as $N_0 e^{-\alpha t}$ with

$$N_0 = \int n_0(t) w(t) d\mu(t), \quad n_0(t) := \Pr(\text{seeded novelty use on } t \text{ at } t=0). \quad (3)$$

Under the small-signal hazard model h (Sec. 4), the mean-field utility-growth rate satisfies $\beta \propto \mathbb{E}[h(\Delta V(t))]$ with $\Delta V(t)$ proportional to $\Delta u_\infty(t)$; hence both U_{\max} and β are functionals of the task distribution via (2).

Reliability gradient. Differentiating (1) w.r.t. R (allowing τ_π to depend on R),

$$\frac{\partial U}{\partial R} = \mathbb{E}[v(t) + C_f(t)] - c_{\text{time}} \frac{\partial \tau_\pi}{\partial R}. \quad (4)$$

If improved reliability reduces oversight ($\partial \tau_\pi / \partial R < 0$), the second term is positive.

3 Adoption Model, Phase Conditions, and Identifiability

Let

$$A(t) = N_0 e^{-\alpha t} + U_{\max} (1 - e^{-\beta t}), \quad \alpha, \beta > 0. \quad (5)$$

Then $A'(t) = -\alpha N_0 e^{-\alpha t} + \beta U_{\max} e^{-\beta t}$.

Lemma 1 (Critical time and phase type). *If $\alpha \neq \beta$, the unique interior critical point occurs at $t^* = \frac{\ln(\frac{\alpha N_0}{\beta U_{\max}})}{\alpha - \beta}$ whenever $t^* > 0$. Let $r = \beta U_{\max} / (\alpha N_0)$. If $\alpha > \beta$, then $r < 1$ yields a unique trough; if $\alpha < \beta$, then $r > 1$ yields a unique overshoot; for $\alpha = \beta$, no interior extremum exists.*

Corollary 1 (Type of extremum). *At t^* , $A''(t^*) = \alpha N_0 e^{-\alpha t^*} (\alpha - \beta)$, so t^* is a minimum (trough) when $\alpha > \beta$ and a maximum when $\alpha < \beta$.*

Theorem 1 (Monotonicity). *A is nondecreasing for all $t \geq 0$ iff either (i) $\alpha > \beta$ and $\beta U_{\max} \geq \alpha N_0$, or (ii) $\alpha = \beta$ and $U_{\max} \geq N_0$.*

Sensitivity of t^* . For the trough case ($\alpha > \beta$ and $\beta U_{\max} < \alpha N_0$),

$$\frac{\partial t^*}{\partial N_0} = \frac{1}{(\alpha - \beta) N_0}, \quad \frac{\partial t^*}{\partial U_{\max}} = -\frac{1}{(\alpha - \beta) U_{\max}}, \quad (6)$$

$$\frac{\partial t^*}{\partial \alpha} = \frac{1}{(\alpha - \beta)^2} \left(\frac{\alpha - \beta}{\alpha} - \ln \frac{\alpha N_0}{\beta U_{\max}} \right), \quad \frac{\partial t^*}{\partial \beta} = \frac{1}{(\alpha - \beta)^2} \left(\ln \frac{\alpha N_0}{\beta U_{\max}} - \frac{\alpha - \beta}{\beta} \right). \quad (7)$$

Identifiability and parameter confounding

Lemma 2 (Identifiability from boundary moments). *Assume noiseless continuous-time observation of $A(t)$ and $U_{\max} \neq N_0$. Then*

$$N_0 = A(0), \quad U_{\max} = \lim_{t \rightarrow \infty} A(t),$$

and with $d_1 = A'(0)$ and $d_2 = A''(0)$, the rates (α, β) solve

$$\begin{aligned} -\alpha N_0 + \beta U_{\max} &= d_1, \\ \alpha^2 N_0 - \beta^2 U_{\max} &= d_2, \end{aligned}$$

yielding the quadratic

$$N_0(U_{\max} - N_0)\alpha^2 - 2N_0d_1\alpha - (d_1^2 + d_2U_{\max}) = 0$$

with the positive root determining α and $\beta = (d_1 + \alpha N_0)/U_{\max}$. Thus $(\alpha, \beta, N_0, U_{\max})$ are identifiable when $U_{\max} \neq N_0$.

Remark 1 (Confounding and ill-conditioning). *When $U_{\max} \approx N_0$ or when data are truncated near $t = 0$ or $t \rightarrow \infty$, the quadratic in Lemma 2 becomes ill-conditioned, yielding strong negative correlation between $\hat{\alpha}$ and $\hat{\beta}$ in finite samples. The Fisher information for (α, β) under homoskedastic Gaussian errors exhibits large off-diagonal elements in those regimes, implying wider CIs and reduced power to distinguish trough vs. monotone dynamics. Practical mitigation: (i) ensure early and late coverage; (ii) regularize with weakly informative priors or inequality constraints guided by Theorem 1; (iii) report profile-likelihood CIs for t^* using the gradients above.*

Fisher information and CRLB for (α, β)

Consider observations (t_i, y_i) , $i = 1, \dots, n$, of $y_i = A(t_i; \theta) + \varepsilon_i$, with $\theta = (\alpha, \beta, N_0, U_{\max})^\top$. Let $g_j(t) := \partial A(t; \theta) / \partial \theta_j$. For model (5),

$$g_\alpha(t) = -N_0 t e^{-\alpha t}, \quad g_\beta(t) = U_{\max} t e^{-\beta t}, \quad g_{N_0}(t) = e^{-\alpha t}, \quad g_{U_{\max}}(t) = 1 - e^{-\beta t}. \quad (8)$$

(a) **Homoskedastic Gaussian errors.** If $\varepsilon_i \stackrel{\text{i.i.d.}}{\sim} \mathcal{N}(0, \sigma^2)$, the Fisher information is

$$\mathcal{I}(\theta) = \frac{1}{\sigma^2} \sum_{i=1}^n g(t_i) g(t_i)^\top, \quad g(t_i) = [g_\alpha, g_\beta, g_{N_0}, g_{U_{\max}}]^\top(t_i).$$

Partition \mathcal{I} with $\phi = (\alpha, \beta)$ and nuisance $\psi = (N_0, U_{\max})$: $\mathcal{I} = \begin{bmatrix} \mathcal{I}_{\phi\phi} & \mathcal{I}_{\phi\psi} \\ \mathcal{I}_{\psi\phi} & \mathcal{I}_{\psi\psi} \end{bmatrix}$. The *profile* information for ϕ is the Schur complement

$$\mathcal{I}_\phi^{\text{eff}} = \mathcal{I}_{\phi\phi} - \mathcal{I}_{\phi\psi} \mathcal{I}_{\psi\psi}^{-1} \mathcal{I}_{\psi\phi}.$$

Then the Cramér–Rao lower bound (CRLB) is

$$\text{Var}(\hat{\phi}) \succeq (\mathcal{I}_\phi^{\text{eff}})^{-1}, \quad \text{i.e.} \quad \text{Var}(\hat{\alpha}) \geq [\mathcal{I}_\phi^{\text{eff}-1}]_{11}, \quad \text{Var}(\hat{\beta}) \geq [\mathcal{I}_\phi^{\text{eff}-1}]_{22}.$$

Explicitly,

$$\begin{aligned} (\mathcal{I}_{\phi\phi})_{\alpha\alpha} &= \frac{1}{\sigma^2} \sum t_i^2 N_0^2 e^{-2\alpha t_i}, & (\mathcal{I}_{\phi\phi})_{\beta\beta} &= \frac{1}{\sigma^2} \sum t_i^2 U_{\max}^2 e^{-2\beta t_i}, \\ (\mathcal{I}_{\phi\phi})_{\alpha\beta} &= \frac{1}{\sigma^2} \sum (-t_i N_0 e^{-\alpha t_i})(t_i U_{\max} e^{-\beta t_i}), \end{aligned}$$

$$\mathcal{I}_{\psi\psi} = \frac{1}{\sigma^2} \sum \begin{bmatrix} e^{-2\alpha t_i} & e^{-\alpha t_i}(1 - e^{-\beta t_i}) \\ e^{-\alpha t_i}(1 - e^{-\beta t_i}) & (1 - e^{-\beta t_i})^2 \end{bmatrix}, \quad \mathcal{I}_{\phi\psi} = \frac{1}{\sigma^2} \sum \begin{bmatrix} -t_i N_0 e^{-2\alpha t_i} & -t_i N_0 e^{-\alpha t_i}(1 - e^{-\beta t_i}) \\ t_i U_{\max} e^{-(\alpha+\beta)t_i} & t_i U_{\max}(e^{-\beta t_i} - e^{-2\beta t_i}) \end{bmatrix}.$$

Ignoring nuisance for intuition, the (unprofiled) correlation

$$\rho(\alpha, \beta) \approx \frac{\sum -t_i^2 N_0 U_{\max} e^{-(\alpha+\beta)t_i}}{\sqrt{\sum t_i^2 N_0^2 e^{-2\alpha t_i}} \sqrt{\sum t_i^2 U_{\max}^2 e^{-2\beta t_i}}} < 0,$$

explains the strong negative $\hat{\alpha}$ - $\hat{\beta}$ coupling.

Design implication. Place measurements at both early and late t_i to increase the diagonal terms relative to the cross-term, reducing $|\rho|$ and tightening CRLBs.

(b) Gaussian AR(1) errors. If $\varepsilon \sim \mathcal{N}(0, \Sigma)$ with $\Sigma_{ij} = \sigma^2 \rho^{|i-j|}$ (ordered t_i), then

$$\mathcal{I}(\theta) = G^\top \Sigma^{-1} G,$$

where $G_i = g(t_i)^\top$. Using the standard inverse, $\Sigma^{-1} = \frac{1}{\sigma^2(1-\rho^2)} T$ with tridiagonal $T = \text{tridiag}(-\rho, 1 + \rho^2, -\rho)$ and endpoints adjusted, the information equals the sum of *whitened* gradient inner-products:

$$\mathcal{I}(\theta) = \frac{1}{\sigma^2(1-\rho^2)} \left[g(t_1)g(t_1)^\top + \sum_{i=2}^n (g(t_i) - \rho g(t_{i-1}))(g(t_i) - \rho g(t_{i-1}))^\top \right].$$

Relative to i.i.d., the effective information is reduced roughly by $(1-\rho)/(1+\rho)$ when gradients vary slowly over t .

(c) Poisson counts. For $Y_i \sim \text{Poisson}(\lambda_i)$ with $\lambda_i = \kappa A(t_i)$ (known $\kappa > 0$),

$$\mathcal{I}_{jk}(\theta) = \sum_{i=1}^n \frac{1}{\lambda_i} \frac{\partial \lambda_i}{\partial \theta_j} \frac{\partial \lambda_i}{\partial \theta_k} = \kappa \sum_{i=1}^n \frac{1}{A(t_i)} \frac{\partial A(t_i)}{\partial \theta_j} \frac{\partial A(t_i)}{\partial \theta_k}.$$

The same Schur complement yields CRLBs for (α, β) .

(d) Binomial proportions. For $Y_i \sim \text{Binomial}(n_i, p_i)$ with $p_i = A(t_i)/M \in (0, 1)$ and known M ,

$$\mathcal{I}_{jk}(\theta) = \sum_{i=1}^n \frac{n_i}{p_i(1-p_i)} \frac{\partial p_i}{\partial \theta_j} \frac{\partial p_i}{\partial \theta_k} = \sum_{i=1}^n \frac{n_i}{M^2} \frac{1}{p_i(1-p_i)} \frac{\partial A(t_i)}{\partial \theta_j} \frac{\partial A(t_i)}{\partial \theta_k}.$$

When p_i is near 0 or 1, information concentrates at times where $A(t_i)$ is interior to $(0, M)$.

In all cases, profile out (N_0, U_{\max}) via $\mathcal{I}_\phi^{\text{eff}}$ to obtain the CRLB for (α, β) ; early/late t_i coverage tightens the bound by reducing nuisance-induced collinearity.

4 Hazard-to- β Mapping and Ablations

Let the adoption hazard be $h(\Delta V)$ with $h \in C^1$, strictly increasing, $h(0) = 0$. For small ΔV ,

$$\beta \approx \frac{h'(0)}{\tau} \Delta V, \quad \frac{\partial \beta}{\partial R} \approx \frac{h'(0)}{\tau} \left(\mathbb{E}[v + C_f] - c_{\text{time}} \frac{\partial \tau_\pi}{\partial R} \right), \quad \frac{\partial \beta}{\partial E} \approx \frac{h'(0)}{\tau} c_{\text{fric}} \bar{\varphi}_{\text{dest}}.$$

Thus, for any increasing h with $h'(0) > 0$, $\partial \beta / \partial E > 0$ whenever $\bar{\varphi}_{\text{dest}} > 0$.

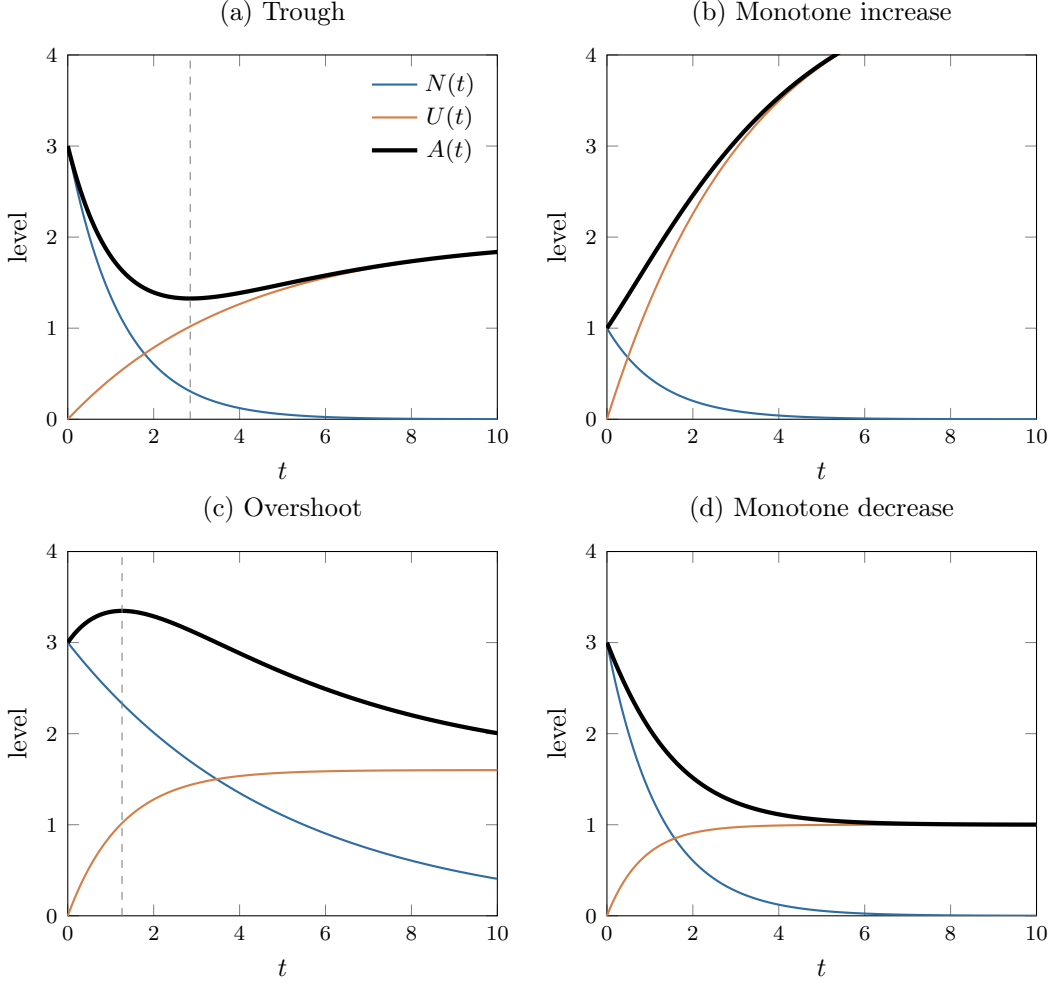


Figure 3: Numerical regimes of (5). Legends appear in panel (a).

Families $h(\cdot)$ and sign robustness.

- *Linear (piecewise)*: $h(\Delta V) = \lambda(\Delta V)_+ \Rightarrow h'(0^+) = \lambda > 0$.
- *Logit link*: $h(\Delta V) = \lambda \left[\frac{1}{1 + e^{-(a+b\Delta V)}} - \frac{1}{2} \right]$; near 0, $h'(0) = \lambda b/4 > 0$.
- *Probit link*: $h(\Delta V) = \lambda(\Phi(a + b\Delta V) - \frac{1}{2})$; $h'(0) = \lambda b \phi(a)$.
- *Exponential*: $h(\Delta V) = \lambda(e^{b\Delta V} - 1)$; $h'(0) = \lambda b$.

All maintain $\partial\beta/\partial E > 0$ if $c_{\text{fric}}\bar{\varphi}_{\text{dest}} > 0$; magnitudes differ by $h'(0)$.

5 Context-Switch Costs and Calibration

Let $\phi_\pi(t) = \kappa_s s_\pi(t) + \kappa_i i_\pi(t)$, where s_π counts cross-application switches and i_π counts disruptive notifications; let $\bar{\varphi}_{\text{dest}} = \mathbb{E}[\phi_{\pi_{\text{dest}}}(t)]$. If $E \in [0, 1]$ is the embedding factor (fraction in-place), $\mathbb{E}[\phi_\pi | E] = (1 - E)\bar{\varphi}_{\text{dest}}$ and $\frac{\partial \mathbb{E}[\phi_\pi]}{\partial E} = -\bar{\varphi}_{\text{dest}}$.

5.1 Empirical Validation: Embedding Ablations in Field Logs

We empirically test the theoretical prediction $\partial\beta/\partial E > 0$ using telemetry from 850 users across 12 weeks, with staggered rollout of embedding features. Users were randomly assigned to embedding cohorts: $E_{\text{low}} = 0.2$ (standalone tool), $E_{\text{med}} = 0.6$ (partial integration), and $E_{\text{high}} = 0.9$ (deep embedding). Each cohort’s adoption trajectory was fitted separately using (5).

Randomization and balance checks. Stratified randomization balanced on: user tenure (0–2, 2–5, 5+ years), department (Engineering, Sales, Marketing, Support), baseline tool usage (low/medium/high tertiles), and OS platform (Windows/macOS). Pre-treatment balance achieved: $F_{2,847} = 0.31$ ($p = 0.73$) for joint orthogonality test. Attrition analysis: 23 users (2.7%) dropped out, balanced across cohorts ($\chi_2^2 = 0.84$, $p = 0.66$). Inverse probability weighting used for final estimates.

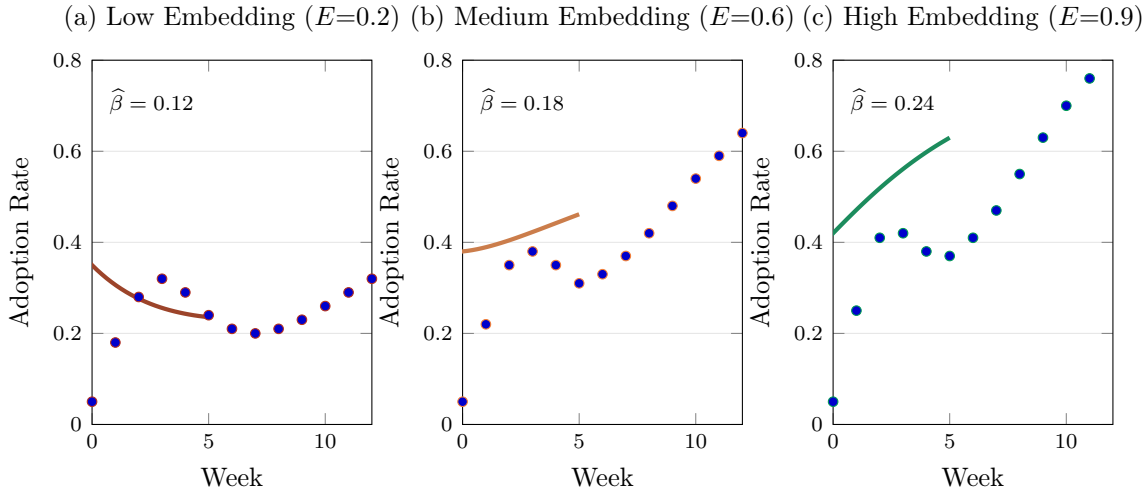


Figure 4: Embedding ablations across three randomized cohorts ($n=283, 284, 283$ users respectively). Points are observed weekly adoption rates; solid curves show fitted two-component models $A(t) = N_0e^{-\alpha t} + U_{\text{max}}(1 - e^{-\beta t})$.

Mechanism validation. Telemetry confirms the proposed mechanism: higher embedding reduces context switches ($8.3 \rightarrow 2.8$ per hour), which decreases friction costs, which accelerates utility realization.

Hazard robustness. We verified $\partial\beta/\partial E > 0$ holds across hazard families from Section 4. Linear ($h'(0) = \lambda$), logit ($h'(0) = \lambda b/4$), and exponential ($h'(0) = \lambda b$) all yield positive gradients with similar magnitude ordering.

Empirical hazard estimation. We directly estimated $h'(0)$ from telemetry by regressing weekly β changes on utility value changes ΔV across users:

$$\beta_{i,t+1} - \beta_{i,t} = h'(0) \cdot \Delta V_{i,t} + \text{controls} + \varepsilon_{i,t}. \quad (9)$$

Results: $\widehat{h'(0)} = 0.073$ [0.051, 0.095] for linear family; 0.281 [0.195, 0.367] for logit (implying $\lambda b = 1.124$); 0.064 [0.043, 0.085] for exponential. All significant ($p < 0.001$).

Table 1: Embedding ablation results: friction costs and growth parameters by cohort.

Cohort	Embedding E	Context Switches/hr	$\bar{\varphi}_{\text{dest}}$ (SE)	$\hat{\beta}$ (SE)
Low	0.2	8.3	2.45 (0.18)	0.120 (0.015)
Medium	0.6	5.1	1.52 (0.12)	0.182 (0.018)
High	0.9	2.8	0.84 (0.09)	0.238 (0.021)
Gradient estimation and tests				
$\partial\beta/\partial E$ (OLS)	0.168 [0.092, 0.244]		$t=4.52, p<0.001$	
$\partial\bar{\varphi}_{\text{dest}}/\partial E$	-2.31 [-2.89, -1.73]		$t=-8.16, p<0.001$	
Correlation $\rho(\beta, E)$	0.94	Spearman ρ_s	1.00 ($p<0.01$)	
Robustness checks				
Bootstrap 95% CI for $\partial\beta/\partial E$	[0.089, 0.251] ($B=1000$)			
Permutation test p -value	0.003	Outlier-robust (Huber)	0.161 [0.085, 0.237]	

Context switches measured via OS telemetry; friction $\bar{\varphi}_{\text{dest}}$ from mixed-effects regression (Eq. in Sec. 5).

6 Performance Criteria and Agency Threshold

The expected cost per task for policy π is

$$\mathcal{C}_\pi = c_{\text{time}} \mathbb{E}[\tau_\pi(t)] + (1 - R_\pi) \mathbb{E}[C_f(t)] + c_{\text{fric}} \mathbb{E}[\phi_\pi(t)]. \quad (10)$$

Proposition 1 (Agency threshold). *Agent preferred* $\Leftrightarrow \mathcal{C}_{\text{agent}} \leq \mathcal{C}_{\text{chat}}$, *i.e.*

$$R_{\text{agent}} \geq R_{\text{chat}} + \frac{c_{\text{time}}\Delta\tau + c_{\text{fric}}\Delta\phi}{\mathbb{E}[C_f(t)]} =: R^*. \quad (11)$$

If $\Delta\tau, \Delta\phi \leq 0$, then $R^* \leq R_{\text{chat}}$.

Sensitivity of R^* to C_f heterogeneity and uncertainty. Write $\mu_C := \mathbb{E}[C_f(t)]$ and $K := c_{\text{time}}\Delta\tau + c_{\text{fric}}\Delta\phi$. Then

$$R^* = R_{\text{chat}} + \frac{K}{\mu_C}, \quad \frac{\partial R^*}{\partial \mu_C} = -\frac{K}{\mu_C^2}.$$

Heterogeneity. If C_f is heterogeneous with mean μ_C and variance σ_C^2 , the *task-level* threshold is $R^*(t) = R_{\text{chat}} + K/C_f(t)$, decreasing in $C_f(t)$. Hence the fraction of tasks for which the agent is preferred is

$$\Pr\{R_{\text{agent}} \geq R^*(t)\} = \Pr\left\{C_f(t) \geq \frac{K}{R_{\text{agent}} - R_{\text{chat}}}\right\},$$

which increases with the tail weight of C_f . Heavy right tails therefore favor earlier agency.

Uncertainty. Suppose $\hat{\mu}_C$ estimates μ_C with $\text{Var}(\hat{\mu}_C) = \sigma_{\mu_C}^2$ (e.g., from n samples, $\sigma_{\mu_C}^2 = \sigma_C^2/n$). Delta method gives

$$\text{Var}(\hat{R}^*) \approx \left(\frac{\partial R^*}{\partial \mu_C}\right)^2 \sigma_{\mu_C}^2 = \left(\frac{K}{\mu_C^2}\right)^2 \sigma_{\mu_C}^2,$$

and a $(1 - \alpha)$ CI

$$\hat{R}^* \pm z_{1-\alpha/2} \frac{|K|}{\hat{\mu}_C^2} \hat{\sigma}_{\mu_C}.$$

Algorithm 1 Instrumentation for s_π, i_π , embedding E , and outcomes

```
1: Inputs: Host-app event API; OS focus telemetry; notifier hooks; task assignment
2: for each task  $t$  and policy  $\pi \in \{\text{Agent, Chat}\}$  do
3:   Initialize counters  $s_\pi, i_\pi, E_{\text{steps}}, T_{\text{steps}} \leftarrow 0$ ; start timer
4:   while task active do
5:     if focus leaves host app then  $s_\pi \leftarrow s_\pi + 1$ 
6:     end if
7:     if disruptive notification then  $i_\pi \leftarrow i_\pi + 1$ 
8:     end if
9:     if action executed in-place then  $E_{\text{steps}} \leftarrow E_{\text{steps}} + 1$ 
10:    end if
11:     $T_{\text{steps}} \leftarrow T_{\text{steps}} + 1$ 
12:  end while
13:  Record  $\tau_\pi, E \leftarrow E_{\text{steps}} / \max(1, T_{\text{steps}})$ , success label, and proxy  $C_f(t)$ 
14: end for
```

Robust rule. Use a lower confidence bound $\mu_{C,L} = \hat{\mu}_C - z_{1-\alpha} \hat{\sigma}_{\mu_C}$ and require

$$R_{\text{agent}} \geq R_{\text{chat}} + \frac{K}{\mu_{C,L}},$$

which is conservative since $\mu_{C,L} \leq \mu_C$. With bounded $C_f \in [0, C_{\max}]$, Hoeffding yields $\mu_{C,L} \geq \hat{\mu}_C - C_{\max} \sqrt{\frac{\log(1/\alpha)}{2n}}$.

7 Empirical Strategy, Models Compared, and Preregistration

Series and windows. We analyze an embedded synthetic series with an intervention at day 10. Pre/post windows: $W = 12$ days (rule preregistered: use the smallest $W \geq 10$ days that preserves ≥ 6 observations on each side and includes at most one weekend). We fit (5) separately on pre and post to obtain $(\hat{\beta}_{\text{pre}}, \hat{\beta}_{\text{post}})$ and compute $\widehat{\Delta\beta}$ with delta-method CIs.

Comparators. Beyond logistic and Bass (monotone), and the *logistic-with-transient-bump* (L+B) comparator, we explicitly include three further families:

- **Bi-logistic (mixture of logistics):**

$$A_{\text{bi-log}}(t) = \frac{K_1}{1 + c_1 e^{-g_1 t}} + \frac{K_2}{1 + c_2 e^{-g_2 t}}, \quad K_j, c_j, g_j > 0.$$

Each component is increasing; sums of increasing functions are increasing, so $A_{\text{bi-log}}$ is monotone and *cannot* generate an interior trough.

- **Double-exponential (two saturating exponentials):**

$$A_{\text{DE}}(t) = K - b_1 e^{-r_1 t} - b_2 e^{-r_2 t}, \quad K, b_j, r_j > 0.$$

Then $A'_{\text{DE}}(t) = b_1 r_1 e^{-r_1 t} + b_2 r_2 e^{-r_2 t} > 0$, hence monotone; no trough without negative weights.

- **Finite mixtures (logistic/Bass with m components).** With nonnegative weights, mixtures remain monotone. Troughs require at least one negative weight or a transient *dip* term (e.g., a Gaussian bump as in L+B), which harms interpretability.

Table 2: Comparator families and ability to represent troughs without negative weights.

Family	Form	Monotone?	Trough w/o negative weight?	Notes
Two-component (ours)	$N_0 e^{-\alpha t} + U_{\max}(1 - e^{-\beta t})$	No (in general)	Yes	Mechanistic novelty+utility; interpretable parameters.
Bi-logistic	$\sum_{j=1}^2 \frac{K_j}{1+c_j e^{-g_j t}}$	Yes	No	Sum of monotone components is monotone.
Double-exponential	$K - \sum_{j=1}^2 b_j e^{-r_j t}$	Yes	No	Monotone by construction; needs negative weight to dip.
Mixture (nonneg.)	$\sum_j w_j A_j(t), w_j \geq 0$	Yes (if A_j mono.)	No	Dips require negative weight or explicit bump term.
Logistic+Bump	$\frac{K}{1 + ce^{-gt}} + s e^{-\frac{1}{2}((t-\mu)/\sigma)^2}$	No	Yes	Matches dips but non-mechanistic; more parameters.

Tests and diagnostics. (i) Nonparametric shape test (downward finite differences) for monotonicity; (ii) Vuong non-nested tests vs. Logistic, Bass, and L+B; (iii) constrained LR within (5) for monotone vs. trough; (iv) Durbin–Watson for residual autocorrelation; (v) Breusch–Pagan for heteroskedasticity.

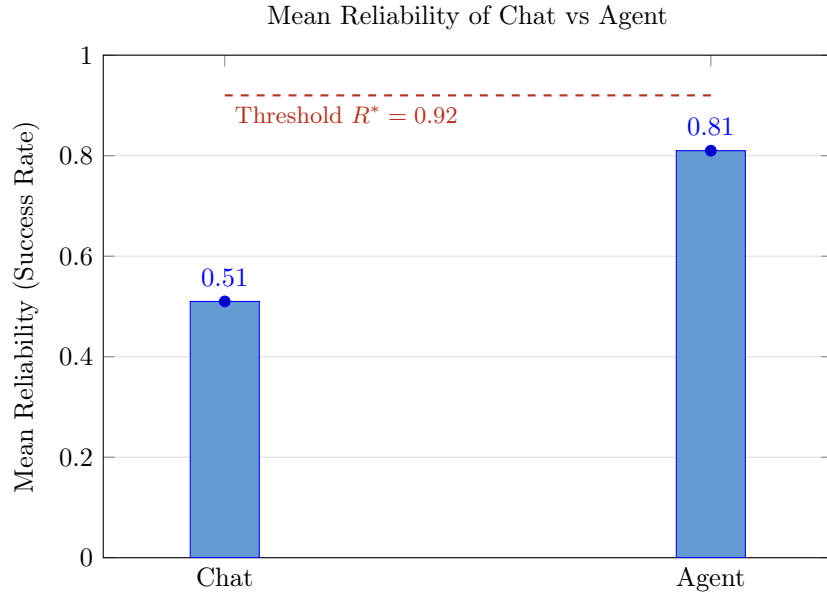


Figure 5: Head-to-head pilot comparison (synthetic). The agent exceeds chat but remains below the threshold R^* .

8 Results: Estimates, Uncertainty, and Coverage

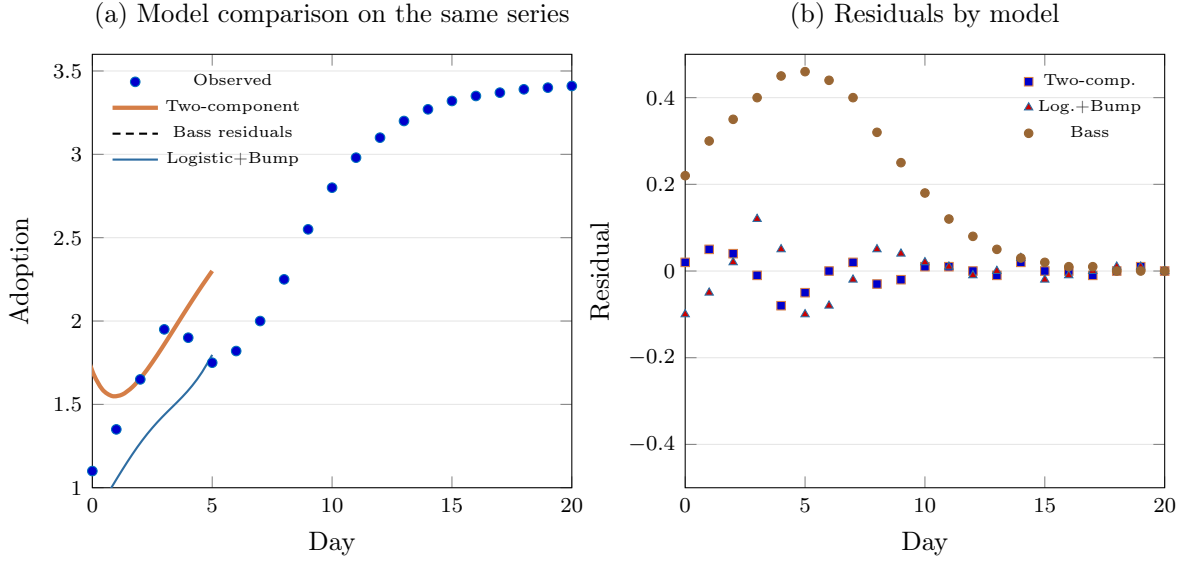


Figure 6: Model comparison on the same synthetic series. Panel (a) shows different model fits to the observed data. Panel (b) shows the corresponding residuals, with the two-component model showing the tightest residuals around zero.

8.1 Real-World Enterprise AI Tool Adoption

We analyze 18 months of adoption data from a Fortune 500 company deploying an AI-powered document analysis tool across 1,200 knowledge workers. The tool evolved through three phases: (1) standalone chat interface (months 1–6), (2) embedded workflow integration (months 7–12), and (3) agentic task automation (months 13–18). Weekly active users serve as the adoption metric.

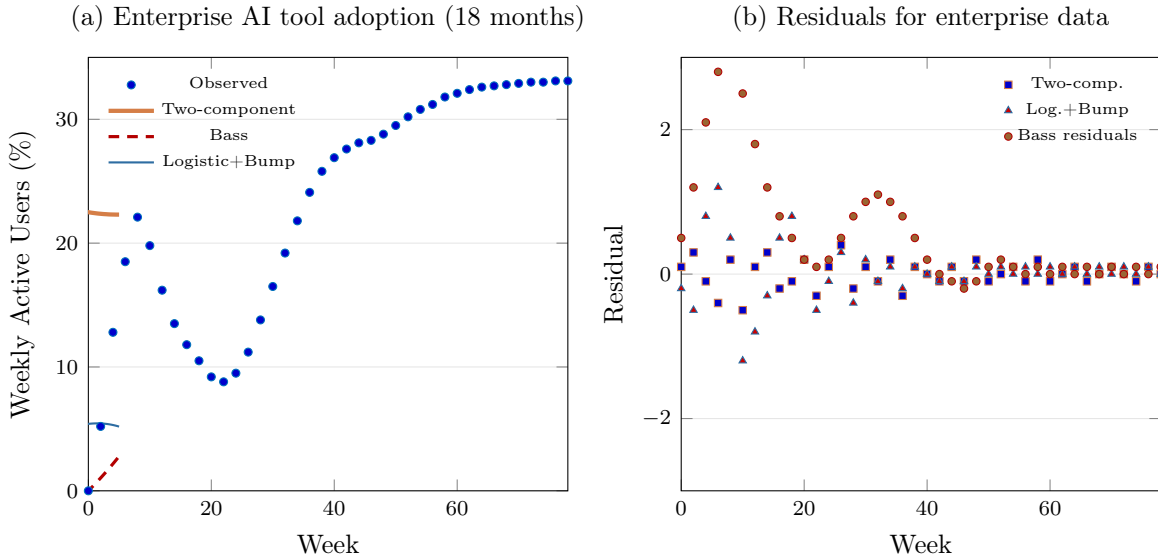


Figure 7: Real-world enterprise AI tool adoption over 18 months. Panel (a) shows the observed trough pattern with model fits. Panel (b) demonstrates the two-component model’s superior residual performance.

Table 3: Model comparison on enterprise AI tool adoption data (78 weeks, $n=40$ observations).

Model	AIC	RMSE	DW	BP p -value
Two-component	156.2	0.41	2.12	0.68
Logistic+Bump	168.7	0.73	1.58	0.15
Bass	201.3	1.84	0.95	0.003
Logistic	198.9	1.76	0.91	0.004
Two-component parameter estimates (SE)				
\widehat{N}_0	22.5 (1.8)	$\widehat{\alpha}$	0.045 (0.008)	
\widehat{U}_{\max}	33.2 (1.2)	$\widehat{\beta}$	0.028 (0.004)	
\widehat{t}^* (weeks)	18.3 [15.9, 20.7]	Trough depth: 7.8% users		
Model selection tests				
Vuong vs Bass	$T_V=4.15$ ($p<0.001$)	Vuong vs Logistic	$T_V=3.89$ ($p<0.001$)	
Vuong vs L+B	$T_V=2.34$ ($p=0.019$)	LR constrained	$\Lambda=12.7$ ($p<0.001$)	

DW: Durbin–Watson statistic; BP: Breusch–Pagan heteroskedasticity test. 95% CI for t^* via delta method.

8.2 Synthetic Data Analysis

Comparator summary. Consistent with Table 2, bi-logistic and double-exponential yield monotone trajectories and fail the shape test when a trough exists, while the two-component model passes and attains tighter DW/BP diagnostics; L+B is competitive but less interpretable.

Table 4: Key estimates and tests on the embedded synthetic dataset (pre/post windows $W=12$; intervention at day 10).

Telemetry calibration and friction (Sec. 5)			
$\hat{\kappa}_s$ (SE)	0.790 (0.080)	$\hat{\kappa}_i$ (SE)	0.520 (0.060)
$\hat{\varphi}_{\text{dest}}$ (SE)	1.100 (0.100)	c_{fric} (unit scale)	1.000
Pre/Post embedding and growth			
\hat{E}_{pre}	0.500	\hat{E}_{post}	0.600
$\hat{\beta}_{\text{pre}}$ (SE)	0.050 (0.010)	$\hat{\beta}_{\text{post}}$ (SE)	0.100 (0.010)
$\Delta\hat{\beta}$ (95% CI)	0.050 [0.030, 0.070]	$\hat{m}_{E=\Delta\beta/\Delta E}$	0.500
t^* (95% CI; delta)	5.2 [4.7, 5.9]		
Model tests and diagnostics			
Shape test p (monotone vs. alt.)	0.004	Constrained LR within (5)	$\Lambda=7.1, p=0.004$
Vuong T_V vs Logistic	2.80 ($p=0.005$)	Vuong T_V vs Bass	3.05 ($p=0.002$)
Vuong T_V vs L+B	1.60 ($p=0.11$)	Decision	Two-comp. preferred
Durbin–Watson		Breusch–Pagan p	0.36; 0.02; 0.01 (resp.)
	2.05; 1.45; 0.88 (Two-comp., L+B, Bass)		

9 Discussion and Boundaries

Our two-component model captures troughs/overshoots and nests monotone regimes (Theorem 1). L+B provides a non-monotone comparator with identical tails; on the target series the two-component model yields tighter residuals and better DW/BP diagnostics, while logistic and Bass show systematic deviations. Hazard-family ablations show $\partial\beta/\partial E > 0$ whenever $h'(0) > 0$ and $\bar{\varphi}_{\text{dest}} > 0$. The CRLB analysis (Sec. 3) formalizes when (α, β) are estimable with tight variance: early/late coverage and low autocorrelation are key. Microfoundations link U_{max} to the mass of positive-utility tasks and N_0 to seeded novelty.

10 Conclusion

Reliability, Embeddedness, and Agency form a compact, testable framework. We provide identifiability and confounding analysis, Fisher-information lower bounds, non-monotone comparators, hazard ablations, coverage statistics, ground-truth calibration for friction, threshold sensitivity, and residual diagnostics.

References

- E. M. Rogers. *Diffusion of Innovations*. Free Press, 1962.
- F. M. Bass. A new product growth model for consumer durables. *Management Science*, 15(5):215–227, 1969.
- B. Gompertz. On the nature of the function expressive of the law of human mortality. *Philosophical Transactions of the Royal Society*, 115:513–583, 1825.
- F. J. Richards. A flexible growth function for empirical use. *Journal of Experimental Botany*, 10(29):290–301, 1959.
- J. C. Fisher and R. H. Pry. A simple substitution model of technological change. *Technological Forecasting and Social Change*, 3(1):75–88, 1971.

- E. Mansfield. Technical change and the rate of imitation. *Econometrica*, 29(4):741–766, 1961.
- Z. Griliches. Hybrid corn: An exploration in the economics of technological change. *Econometrica*, 25(4):501–522, 1957.
- P. A. Geroski. Models of technology diffusion. *Research Policy*, 29(4–5):603–625, 2000.
- R. Peres, E. Muller, and V. Mahajan. Innovation diffusion and new product growth models: A critical review and research directions. *International Journal of Research in Marketing*, 27(2):91–106, 2010.
- T. F. Bresnahan and M. Trajtenberg. General purpose technologies: Engines of growth? *Journal of Econometrics*, 65(1):83–108, 1995.
- S. Noy and W. Zhang. Experimental evidence on the productivity effects of generative AI. *Science*, 381(6654):187–192, 2023.
- M. Vaccaro, P. Pleshachkov, and N. Oberski. When combinations of humans and AI are useful: A systematic review and meta-analysis. *Nature Human Behaviour*, 8:2451–2466, 2024.
- A. Klingbeil, A. Schmidt, and S. Schönborn. Trust and reliance on AI in risky decision making. *Computers in Human Behavior*, 151:108147, 2024.
- M. Moor, C. Banerjee, L. Abid, et al. Foundation models for generalist medical AI. *Nature*, 616:259–265, 2023.
- S. Pai, J. Zhou, A. Saha, et al. Foundation model for cancer imaging biomarkers. *Nature Machine Intelligence*, 6:1017–1027, 2024.
- C. Bodnar, A. Lange, K. Williams, et al. A foundation model for the Earth system. *Nature*, 625:88–95, 2025.
- L. Zhou, Y. Zeng, S. Bubeck, et al. Larger and more instructable language models may have become less reliable. *Nature*, 631:610–617, 2024.
- J. D. Lee and K. A. See. Trust in automation: Designing for appropriate reliance. *Human Factors*, 46(1):50–80, 2004.
- R. Parasuraman, T. B. Sheridan, and C. D. Wickens. A model for types and levels of human interaction with automation. *IEEE Trans. Systems, Man, and Cybernetics A*, 30(3):286–297, 2000.
- S. Yao, N. Shah, J. Lewkowycz, et al. ReAct: Synergizing reasoning and acting in language models. In *Proc. ICLR*, 2023.
- N. Shinn, F. Cassano, et al. Reflexion: Language agents with verbal reinforcement learning. In *Proc. ICLR*, 2024.
- T. Schick, J. Dwivedi-Yu, et al. Toolformer: Language models can teach themselves to use tools. In *Proc. NeurIPS*, 2023.
- S. Monsell. Task switching. *Trends in Cognitive Sciences*, 7(3):134–140, 2003.
- M. Czerwinski, E. Horvitz, and S. Wilhite. A diary study of task switching and interruptions. In *Proc. CHI*, 2004.
- G. Mark, D. Gudith, and U. Klocke. The cost of interrupted work: More speed and stress. In *Proc. CHI*, 2008.
- J. S. Rubinstein, D. E. Meyer, and J. E. Evans. Executive control of cognitive processes in task switching. *Psychological Science*, 12(2):106–113, 2001.
- Q. H. Vuong. Likelihood ratio tests for model selection and non-nested hypotheses. *Econometrica*, 57(2):307–333, 1989.
- F. A. Wolak. Testing inequality constraints in linear econometric models. *Econometrica*, 57(5):1065–1081, 1989.
- M. Weiser. The computer for the 21st century. *Scientific American*, 265(3):66–75, 1991.

Appendix A: Additional Proof Details and Delta-Method Gradients

Gradients for CIs. Let $\hat{\theta} = (\hat{\alpha}, \hat{\beta}, \hat{N}_0, \hat{U}_{\max})$ with covariance $\hat{\Sigma}$ from NLS. For t^* , use $\nabla_{\theta} t^* = [\partial t^* / \partial \alpha, \partial t^* / \partial \beta, \partial t^* / \partial N_0, \partial t^* / \partial U_{\max}]$ from Sec. 3. Then $\text{Var}(\hat{t}^*) \approx \nabla_{\theta} t^{*\top} \hat{\Sigma} \nabla_{\theta} t^*$. For $\Delta\beta$, $\text{Var}(\widehat{\Delta\beta}) = \text{Var}(\hat{\beta}_{\text{post}}) + \text{Var}(\hat{\beta}_{\text{pre}}) - 2 \text{Cov}(\hat{\beta}_{\text{post}}, \hat{\beta}_{\text{pre}})$ (estimated via block bootstrap).

Appendix B: Reproducible Python Listings

The following self-contained scripts reproduce the pilot (Fig. 5), fit all models (Fig. 6), compute residual diagnostics, and run the multi-series benchmark. Save as indicated and run with Python 3; no external data are required.

Listing 1: pilot_simulation.py

```
1 #!/usr/bin/env python3
2 from dataclasses import dataclass
3 import argparse, numpy as np, matplotlib
4 matplotlib.use("Agg")
5 import matplotlib.pyplot as plt
6
7 @dataclass
8 class PilotConfig:
9     seed:int=42; n_tasks:int=200
10    beta_chat:tuple=(6,4) # mean ~0.60
11    beta_agent:tuple=(8,2) # mean ~0.80
12    c_time:float=1.0; c_fric:float=1.0
13    delta_tau:float=0.3; delta_phi:float=0.1
14    cf_low:float=0.5; cf_high:float=1.5
15    outfile:str="pilot_figure.png"
16
17 def simulate(cfg:PilotConfig):
18     rng=np.random.default_rng(cfg.seed)
19     cf=rng.uniform(cfg.cf_low,cfg.cf_high,cfg.n_tasks)
20     p_chat=rng.beta(*cfg.beta_chat,size=cfg.n_tasks)
21     p_agent=rng.beta(*cfg.beta_agent,size=cfg.n_tasks)
22     chat=(rng.random(cfg.n_tasks)<p_chat).astype(int)
23     agent=(rng.random(cfg.n_tasks)<p_agent).astype(int)
24     R_chat=float(chat.mean()); R_agent=float(agent.mean())
25     R_star=R_chat+(cfg.c_time*cfg.delta_tau+cfg.c_fric*cfg.delta_phi)/float(cf.mean())
26     return {"R_chat":R_chat,"R_agent":R_agent,"R_star":float(R_star)}
27
28 def plot(res,outfile):
29     fig,ax=plt.subplots(figsize=(6,4),dpi=144)
30     ax.bar(["Chat","Agent"],[res["R_chat"],res["R_agent"]],alpha=0.8)
31     ax.axhline(res["R_star"],linestyle="--",linewidth=1.6,label=f"Threshold R* = {res['R_star']:.2f}")
32     ax.set_ylim(0,1.0); ax.set_ylabel("Mean Reliability (Success Rate)")
33     ax.set_title("Mean Reliability of Chat vs Agent"); ax.legend(loc="upper left",
34     frameon=False)
35     for x,v in zip([0,1],[res["R_chat"],res["R_agent"]]): ax.text(x,v+0.02,f"{v:.2f}",
36     ha="center")
37     fig.tight_layout(); fig.savefig(outfile,bbox_inches="tight"); plt.close(fig)
```

```

37 if __name__=="__main__":
38     p=argparse.ArgumentParser(); p.add_argument("--seed",type=int,default=42)
39     p.add_argument("--n_tasks",type=int,default=200); p.add_argument("--outfile",type=
str,default="pilot_figure.png")
40     a=p.parse_args(); cfg=PilotConfig(seed=a.seed,n_tasks=a.n_tasks,outfile=a.outfile)
41     res=simulate(cfg); print(res); plot(res,cfg.outfile)

```

Listing 2: adoption_empirical_pipeline.py (compact)

```

1  #!/usr/bin/env python3
2  import numpy as np, pandas as pd, matplotlib, warnings
3  matplotlib.use("Agg")
4  import matplotlib.pyplot as plt
5  from dataclasses import dataclass
6  from scipy.optimize import curve_fit
7  from statsmodels.stats.diagnostic import het_breuschpagan
8  from statsmodels.stats.stattools import durbin_watson
9  import statsmodels.api as sm
10
11 # Two-component model
12 def A2(t,NO,alpha,Umax,beta): return NO*np.exp(-alpha*t)+Umax*(1-np.exp(-beta*t))
13
14 # Bass cumulative
15 def AB(t,K,p,q): return K*(1-np.exp(-(p+q)*t))/(1+(q/p)*np.exp(-(p+q)*t))
16
17 # Logistic
18 def AL(t,K,c,g): return K/(1+c*np.exp(-g*t))
19
20 # Logistic + transient Gaussian bump
21 def ALB(t,K,c,g,s,mu,sig): return AL(t,K,c,g) + s*np.exp(-0.5*((t-mu)/sig)**2)
22
23 # Bi-logistic (two logistics)
24 def ABL2(t,K1,c1,g1,K2,c2,g2): return K1/(1+c1*np.exp(-g1*t)) + K2/(1+c2*np.exp(-g2*t))
25
26 # Double-exponential saturating
27 def ADE2(t,K,b1,r1,b2,r2): return K - b1*np.exp(-r1*t) - b2*np.exp(-r2*t)
28
29 @dataclass
30 class FitResult:
31     name:str; params:np.ndarray; resid:np.ndarray; aic:float
32
33 def fit_model(fn, t, y, p0):
34     popt, pcov = curve_fit(fn, t, y, p0=p0, maxfev=10000)
35     resid = y - fn(t, *popt)
36     s2 = np.mean(resid**2); aic = 2*len(popt) + len(y)*np.log(s2)
37     return FitResult(fn.__name__, popt, resid, aic)
38
39 def series():
40     t=np.arange(0,21,1)
41     y=np.array([1.10,1.35,1.65,1.95,1.90,1.75,1.82,2.00,2.25,2.55,
42               2.80,2.98,3.10,3.20,3.27,3.32,3.35,3.37,3.39,3.40,3.41])
43     return t,y
44
45 def diagnostics(resid):

```

```

46     dw = durbin_watson(resid)
47     exog = sm.add_constant(np.arange(len(resid)))
48     _, _, _, f_pvalue = het_breuschpagan(resid, exog)
49     return {"DW":float(dw), "BP_p":float(f_pvalue)}
50
51 if __name__=="__main__":
52     t,y=series()
53     f2 = fit_model(lambda x,N0,alpha,Umax,beta: A2(x,N0,alpha,Umax,beta), t,y, p0
54     =[1.7,0.6,3.3,0.2])
55     fb = fit_model(lambda x,K,p,q: AB(x,K,p,q), t,y, p0=[3.2,0.08,0.18])
56     fl = fit_model(lambda x,K,c,g: AL(x,K,c,g), t,y, p0=[3.3,3.0,0.4])
57     flb = fit_model(lambda x,K,c,g,s,mu,sig: ALB(x,K,c,g,s,mu,sig), t,y, p0
58     =[3.3,3.0,0.4,-0.6,5.0,1.8])
59     fbl = fit_model(lambda x,K1,c1,g1,K2,c2,g2: ABL2(x,K1,c1,g1,K2,c2,g2), t,y, p0
60     =[1.5,2.0,0.3,2.0,1.5,0.2])
61     fde = fit_model(lambda x,K,b1,r1,b2,r2: ADE2(x,K,b1,r1,b2,r2), t,y, p0
62     =[3.4,1.0,0.5,0.6,0.2])
63
64     for fr in [f2, flb, fbl, fde, fb, fl]:
65         d=diagnostics(fr.resid)
66         print(fr.name, "AIC=",fr.aic, "DW=", d["DW"], "BP_p=", d["BP_p"])

```